SIXTH EUROPEAN ROTORCRAFT AND POWERED LIFT AIRCRAFT FORUM

Paper No. 48

SEMI-EMPIRICAL MODEL FOR THE DYNAMIC STALL OF AIRFOILS IN VIEW OF THE APPLICATION TO THE CALCULATION OF RESPONSES OF A HELICOPTER BLADE IN FORWARD FLIGHT

C. T. Tran, D. Petot

Research Engineers, Structure Department, ONERA

Office National d'Etudes et de Recherches Aérospatiales (ONERA)
92320 Châtillon (France)

September 16-19, 1980
Bristol, England

THE UNIVERSITY, BRISTOL, BS8 1 HR, ENGLAND

SEMI-EMPIRICAL MODEL FOR THE DYNAMIC STALL OF AIRFOILS IN VIEW OF THE APPLICATION TO THE CALCULATION OF RESPONSES OF A HELICOPTER BLADE IN FORWARD FLIGHT

by C. T. Tran & D. Petot

Office National d'Etudes et de Recherches Aérospatiales (ONERA)
92320 Châtillon (France)

ABSTRACT

A system of differential equations relating the aerodynamic forces and the variables defining the velocity of the airfoil section is employed to simulate the time delay effects of the flow. The model involves a number of identifications of the test results of the 2-D airfoil in static and in small amplitude harmonic oscillation or random vibration configurations. Tests at high amplitude motions then permits a verification of the validity of the model.

INTRODUCTION

Boundary layer separations have predominant effects on the unsteady aerodynamics of airfoil sections operating at high incidence, notably on fixed-wing aircraft manœuvring at high lift, on jet-turbine blades and on helicopter blades at high advance ratio.

There is presently no theoretical approach capable to predict the unsteady aerodynamic forces acting on airfoils working in the vicinity or beyond the dynamic stall angle of attack. But the existing numerous wind-tunnel tests on oscillating airfoils do provide a valuable experimental basis for establishing phenomenological models through which certain semi-empirical prediction can be made. Some such models had been elaborated both in the United States and in Great Britain to synthesize, with relatively simple equations, the lift and moments measured on helicopter profiles executing harmonic oscillations, for various values of the parameters defining the motion and the fluid flow (Mach & Reynolds numbers, frequency and amplitude of oscillation, mean incidence, location of pitch axis, etc.) [1], [2], [3].

In the case of helicopters, dynamic stall occurs on the retreating blade (which operates at high incidence in order to compensate its relatively low velocity with respect to the fluid). Such local stall can aggravate the blade stress and can even induce phanomena analogous to instability (stall-flutter).

The complexity of the blade motion (which results from the composition of forward and rotational velocities, variation of cyclic pitch, blade flap and lead-lag and elastic deflexions), added to the presence of flow separation, render the aeroelastic analysis particularly difficult.

For several years, ONERA in collaboration with the SNIAS have made considerable efforts in this field. Methods of calculation had been developed in the linear domain, in which the evaluation of the aerodynamic forces is based on the linear three-dimensional lifting surface theory. The effects of high incidence are accounted for in a semi-empirical manner by introducing the induced incidence, thus allowing to dissociate, for each airfoil section, the effect of two-dimensional separated flow, which can be evaluated by a phenomenological model, from the effect of three-dimensional interaction, which is deduced by a linear calculation (4), (5). Some encouraging results, yet insufficient, had been obtained by the model of the reference 6.

In order to achieve further improvement, ONERA has undertaken to establish a model (7) more suited than the preceding ones and which makes use of the properties of differential equations to simulate the effects of time history (or memory) of the flows. The model is formulated in the time domain and may therefore be applied to all arbitrary motions of the airfoil. The identification of the coefficients of the model's equations requires only the wind-tunnel tests on airfoils in static and in small amplitude harmonic oscillations or random vibration.

1. MODEL FORMULATION

Consider an airfoil of span L , and of constant cross section and chord c in two dimensional flow. Reference velocities and aerodynamic forces will be referred to the fore-quarter chord line (fig.1).

The aerodynamic forces are to be expressed as functions of the velocity $\vec{V}$ of the airfoil with respect to the still air. This velocity can be decomposed into a constant velocity $\vec{V_0}$ and a velocity $\vec{V_1}$ which may be unsteady. If the airfoil represents a helicopter blade section, for instance, $\vec{V_0}$ is the constant rotational speed around the shaft, while $\vec{V_1}$ results from the composition of the forward translational velocity, blade flap, its in-plane oscillation and elastic vibration.

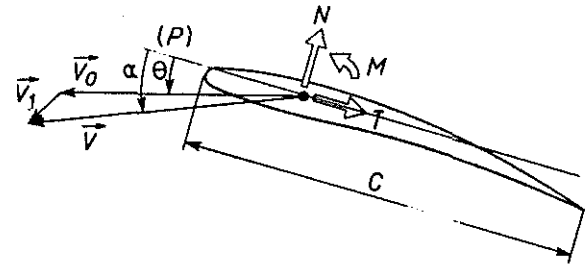

Fig. 1 – Conventions.

The angle α between the velocity $\vec{V}$ and the plane (P) tangent to the airfoil section is the instantaneous aerodynamic incidence at the fore-quarter chord.

Assuming rigid body motion of the airfoil, one can deduce the speed at all points of the chord knowing the velocity $\vec{V}$ and the oscillating pitch velocity $d\theta/dt$, θ being the angular coordinate in pitch, that is, the angle made between the plane (P) and the constant velocity vector $\vec{V_0}$.

The aerodynamic forces resulting from the motion of the airfoil can be defined by the normal lift component N , the tangential force component T and the pitching moment M .

These components will be written in non-dimensional form with reference to the quantities $|V_0|$, c and L .

$$\phi_1 = \frac{N}{1/2\,\rho\,|V_0|^2 c\,L} \qquad \text{normal lift coefficient}$$

$$\phi_2 = \frac{T}{1/2\,\rho\,|V_0|^2 c\,L} \qquad \text{tangential force coefficient}$$

$$\phi_3 = \frac{M}{1/2\,\rho\,|V_0|^2 c^2 L} \qquad \text{pitching moment coefficient}$$

$$\sigma = \frac{|V|}{|V_0|} \qquad \text{velocity ratio}$$

$$\zeta = \frac{|V|\,t}{c} \qquad \text{reduced time}$$

The symbol ($\cdot$) will designate the differentiation with respect to ζ .

The motion of the airfoil with respect to the still fluid is defined by the three functions: $\sigma(\zeta)$, $\alpha(\zeta)$ and $\dot{\theta}(\zeta)$. The velocity ratio σ is directly proportional to the Mach number and as such plays the same rôle in describing the compressibility effect. The values of the functions ϕ_K at the reduced time ζ depend on the time history (since the time $u = -\infty$ up to $u = \zeta$) of σ , α , $\dot{\theta}$ and their successive derivatives. The time history effect of the flow is due to the wake interaction and the delays in the evolution of flow separation and the propagation of acoustic waves.

To create a semi-empirical model implies the formulation of a system of equations of which the solutions ϕ_K depend, in the same manner, on the time-history of the variables σ , α , $\dot{\theta}$ and their successive derivatives. The model will involve a certain number of coefficients which are to be determined by *identification* through experiments. A classical way of introducing the history effect consists of writing a set of differential equations. Since there are three unknowns (ϕ_K , K = 1, 2, 3), the system can be reduced to three interdependent equations :

$$A_r(\cdots \phi_K \cdots,\ \sigma,\ \alpha,\ \dot{\theta},\ \cdots \dot{\phi}_K \cdots,\ \dot{\sigma},\ \dot{\alpha},\ \ddot{\theta},\ \cdots) = 0 \qquad (1.1)$$

$$r = 1, 2, 3$$

The system (1.1) is non linear, since it is designed to simulate the effects of large incidence which are highly non linear.

It will be assumed that the derivatives to be considered may be restricted to a finite order.

Remarks

For practical reasons, the unsteady movements of an airfoil are unfailingly limited in either amplitude or in frequency ; large amplitude motions can only be performed at low frequency and motions at high frequency can only be at small amplitude. It then results that $\dot{\sigma}$, $\dot{\alpha}$, $\dot{\theta}$, $\dot{\phi}_K$ and their derivatives of higher order are small compared to unity.

This can be illustrated, for example, by evaluating the variation of σ resulting from the

composition of the rotational and advancing flight velocities of a helicopter blade. The resolved velocity at a blade section located at the radial distance r is given by $V = \Omega r + U \sin \Omega t$, Ω being the angular velocity and U the advancing flight speed. The constant part Ωr may be assimulated to the vector $\overrightarrow{V_0}$ of figure (1) and the periodic term $U \sin \Omega t$ to the vector $\overrightarrow{V_1}$. The reduced quantities τ and σ in this case are :

$$\tau = \frac{\Omega r t}{c} \quad , \qquad \sigma = \frac{\Omega r + U \sin \Omega t}{\Omega r}$$

then

$$\dot{\sigma} = \frac{d\sigma}{d\tau} = \mu . \frac{c}{r} \cos \frac{c}{r} \tau$$

where μ is the ratio $\frac{U}{\Omega r}$

Excepting the inboard blade sections, both μ and c/r are less than unity. It can then be deduced that $\dot{\sigma} << 1$.

Regarding the variation of the aerodynamic forces, one observes in most cases that the unsteady aerodynamic forces ϕ_K arising from the oscillatory motion of an airfoil deviate only slightly from their static characteristics ϕ_{K0}. It will therefore be assumed, at least provisionally, that the difference between the unsteady and the static aerodynamic forces ($\phi_K - \phi_{K0}$) are small quantities.

Under such conditions, and admitting that the equations A_r are differentiable (*), equation (1.1) can be written as :

$$A_r(P_0) + \sum_K A_{r\phi_K} (\phi_K - \phi_{K0}) + A_{r\dot{\phi}_K} \dot{\phi}_K + \cdots + A_{r\dot{\theta}} \dot{\theta} + A_{r\dot{\alpha}} \dot{\alpha} + \\ + A_{r\dot{\sigma}} \dot{\sigma} + \cdots = 0 \qquad (1.2)$$

P_0 being the n-tuple $P_0 (\ldots \phi_{K0} \ldots, \sigma, \alpha, 0, \ldots)$, with ϕ_{K0} the static value of ϕ_K, where $\dot{\sigma}, \dot{\alpha}, \dot{\theta}, \dot{\phi}_K, \ldots = 0$, and $A_{r\phi_K}, A_{r\dot{\phi}_K} \ldots A_{r\dot{\theta}} \ldots$ the partial derivatives dependent on ϕ_{K0}, σ and α .

$A_r(P_0)$ is the system of equations defining the ϕ_K as functions of σ and α in stationary configurations. Classically, the aerodynamic forces are determined by the coefficients defined by :

$$\begin{vmatrix} N \\ T \\ M \end{vmatrix} = \tfrac{1}{2} \rho \, |V_0|^2 c^2 L \begin{vmatrix} C_1 \\ C_2 \\ C_3 \end{vmatrix}$$

The coefficients C_r are functions of incidence α and Mach number, but the latter is proportional to σ , one thus has :

$$\phi_{r0} = C_r(\alpha, \sigma) \qquad (2.1)$$

The coefficients $C_r(\alpha, \sigma)$ are deduced from wind-tunnel static tests for various incidences and flow speeds.

(*) Wind-tunnel experiments on oscillating airfoils have confirmed that the principle of superposition applies sufficiently well to small amplitude oscillations, even in the case of high incidence. This result justifies the hypothesis on the differentiability of the A_r .

(2.1) allows the writing of the stationary limit of the equations A_r :

$$A_r(P_0) = \phi_{r0} - C_r(\alpha, \sigma) = 0$$

and the equation (1.2) become :

$$\sum_K A_{r\phi_K} \phi_K + A_{r\dot{\phi}_K} \dot{\phi}_K + \cdots = \sum_K A_{r\phi_K} C_K(\alpha,\sigma) - A_{r\dot{\theta}} \dot{\theta} - A_{r\dot{\alpha}} \dot{\alpha} - \cdots \quad (3)$$

The system (3) constitutes a set of linear differential equations with respect to ϕ_K, $\dot{\phi}_K$, $\ddot{\phi}_K$, . . . with variable coefficients, since all partial derivatives are functions of α and σ . The right hand sides are functions of time dependent on the airfoil motion through the functions $\dot{\theta}(\tau)$, $\alpha(\tau)$ and $\sigma(\tau)$.

The resolution of this system of equations is facilitated by the linearity of the left hand sides. However, the hypothesis on the evolution of the forces ϕ_K , which has enabled the present linearisation, is not perfectly verified in circumstances where the airfoil executes motions with large variation in incidence in the stall regime. In such events, it is probable that the unsteady aerodynamic forces may deviate much from their stationary values. Ultimately, it can only be through the comparison with experiments that will justify the linearisation of the equations with respect to ϕ_K .

1.1. Form of the Solutions, Time History Effect

If the motion of the airfoil is imposed, the functions $\dot{\theta}$, α and σ are given functions of τ, and the right hand sides of equations (3) can equally be written as functions of τ , thus of $S_r(\tau)$ .One then has :

$$\sum_K A_{r\phi_K} \phi_K + A_{r\dot{\phi}_K} \dot{\phi}_K + \cdots = S_r(\tau) \quad (4)$$

Let us neglect, for the moment, the variations of the coefficients $A_{r\phi_K}$ . . . with α and σ . This being legitimate while α and σ differ only slightly from their mean values, that is the unsteady motion is of small amplitude.

In this case, the solutions of the equations (4) are formulated by an integral of superposition of impulsive responses :

$$\phi_r(\tau) = \int_{-\infty}^{\tau} G_{rK}(\tau - u)\, S_K(u)\, du \quad (5.1)$$

where $G_r(\tau)$ is the matrix of impulsive responses determined from the left hand side of equation (4).

The solution (5.1) then depends on the evolution of the functions in elapsed time ($u \leq \tau$), which therefore expresses well an effect of time-history.

The effect of history subsists if the coefficients are dependent on $\alpha(\tau)$ and $\sigma(\tau)$. In this case the solution may be written as :

$$\phi_r(\tau) = \int_{-\infty}^{\tau} G_{rj}(\tau)\, G_{jK}(u)\, S_K(u)\, du \qquad (5.2)$$

With $G(\tau)$ now the transition matrix of the left hand side of equations (4).

The matrix G appearing in (5.1) is a superposition of the eigen-solutions of the homogeneous set of equations (4). One has :

$$G(\tau) = \sum_K \Pi_K e^{P_K \tau}$$

where the exponents P_K are the roots of the characteristic equation :

$$\det\left(A_{i\phi_j} + P A_{i\dot{\phi}_j} + P^2 A_{i\ddot{\phi}_j} + \cdots\right) = 0$$

and Π_K are constant matrices.

Remarks

The P_K are also the poles of the transfer function matrix of the homogeneous set of equations (4). The character of the transient responses following the variations of the right hand side of (4) depends on the nature of these poles. The stability of the flow requires that they should be real and negative or complex-conjugates with negative reel parts.

The harmonic responses, that is the modulus and phase of the aerodynamic forces resulting from a harmonic oscillation of the airfoil, depend also fundamentally on the nature of the poles P_K . A real and negative pole leads to continuous and monotonous evolutions of the responses in terms of the frequency of the motion. Whereas, two complex-conjugate poles give rise to solutions that are similar to a structural vibrating system, with rapid evolutions of the modulus and phase in the vicinity of the « resonance frequency ».

These remarks facilitate the identification of the coefficients in the left hand side of equations (3).

1.2. Simplification and Identification of the Model

Equations (3) define the mathematical form of the model apt to simulate the evolution of the aerodynamic forces on an airfoil executing arbitrary unsteady motions. Prior to setting up the model, one must specify the order of the derivatives to be retained, and eventually, bring in some simplification by neglecting certain coefficients or in assuming them to be constant. A series of wind-tunnel identification tests are then performed to determine the numerical values of the remaining coefficients.

The possible simplifications should be founded on experimental comparisons and on physical considerations. The model should correctly interpret the tendencies observed in wind-tunnel tests, and chiefly those that have an influence on aeroelastic couplings. Nevertheless, it would be illusive to attempt to restitute with great precision the whole of the wind-tunnel test results by means of the model.

The experience recently acquired at ONERA (7), justifies the following simplifications :

a) the derivatives of α ; σ and θ of order higher than two may be neglected in the right hand side ;

b) the coefficients in the left hand side which ensure the coupling between the forces ϕ_K may be neglected ($A_{r\phi_K}$, $A_{r\dot{\phi}_K}$, . . . = 0 for $r \neq K$) ;

c) in general one single real pole and two complex-conjugate poles suffice to restitute correctly the evolution of harmonic responses in terms of frequencies.

One then admits that the equations (3) can be decoupled (according to *b*), and that each component ϕ_K can be described by a differential equation of the 3rd order, with a right hand side :

$$A_{r\phi_r}\phi_r + A_{r\dot{\phi}_r}\dot{\phi}_r + A_{r\ddot{\phi}_r}\ddot{\phi}_r + A_{r\dddot{\phi}_r}\dddot{\phi}_r = C_r(\alpha, \sigma) - A_{r\dot{\theta}}\dot{\theta} - A_{r\dot{\alpha}}\dot{\alpha} - A_{r\dot{\sigma}}\dot{\sigma} - A_{r\ddot{\theta}}\ddot{\theta} - A_{r\ddot{\alpha}}\ddot{\alpha} - A_{r\ddot{\sigma}}\ddot{\sigma} \qquad (6)$$

Equations (5.1) which gave the solutions for small amplitude motions become in this case :

$$\phi_r(\tau) = \int_{-\infty}^{\tau} G_r(\tau - u)\, S_r(u)\, du \qquad \text{(without summation)}$$

The measurements of static lift, dray and moment, at different incidences, give the numerical values of C_r . A least square curve fitting procedure then supplies approximate analytical formulae of the C_r which are more convenient to handle than numerically tabulated values. These formulae in general involve two domains of definition : the linear domain and the stall domain. At the boundary between the two, continuity of the functions and of their derivatives must be insured.

Identification of the other coefficients of equations (6) necessitates unsteady flow testing. Since the coefficients are partial derivatives, they can be determined by measurements at small amplitude motions. It is particularly convenient to make the airfoil perform random or simple harmonic oscillation according to the various, degrees of freedom of pitch, plunge or in-plane motions. The in-plane oscillations are particularly useful in the case of helicopter blades where the derivatives with respect to $\dot{\sigma}$ can play a significant role. With regard to the plunging motion, Ref. (8) showed, apart from extreme cases of high amplitude and frequency, the equivalence between plunge and pitch oscillations. The unsteady effects of the two motions may therefore be superimposed.

For identification purpose, tests in pitch oscillation are conducted in the range of the reduced frequency $k = \dfrac{\omega c}{2\,|V_0|}$ corresponding to the domain of application, for example, $0 < k < 1$.

Variations of the coefficients due to the poles have the tendency to be attenuated as the oscillating frequency increases. Tests at high frequency can be exploited to determine the derivatives with respect to $\dot{\theta}$, $\dot{\alpha}$, $\dot{\sigma}$, . . . and tests at low frequency allow identification of the poles.

The measurements conducted on airfoils with large amplitude oscillations are not used for identification, but serve to check the validity of the model after identification.

2. APPLICATION TO THE LINEAR DOMAIN

The model, applied to the case of an infinitely thin airfoil oscillating at small incidence, leads to the synthesis of the results derived from the linear theory of the two-dimensional, unsteady, inviscid flow in harmonic motion, which are published in the form of tables of coefficients by different authors (ref. 9, for example).

Figure 2 specifies the classical notation used to define these coefficients. The position of the airfoil is defined by the pitch angle θ , and the plunge motion h . There is no in-plane mouvement.

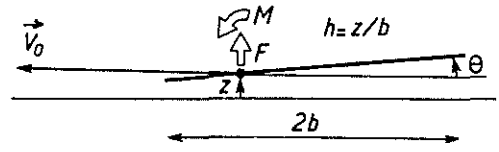

Fig. 2 – Notations used in the thin airfoil linear theory.

$\vec{V_0}$ is the upstream velocity. The deflections h and θ being considered as infinitely small, it is deduced that σ is equal to 1 up to the 2nd order.

The unsteady harmonic motion is defined by :

$$\begin{vmatrix} h(\tau) \\ \theta(\tau) \end{vmatrix} = \begin{vmatrix} \tilde{h} \\ \tilde{\theta} \end{vmatrix} e^{ik\tau}$$ (the real part $R_e(\ldots)$ being implied)

with k the reduced angular frequency.

The lift and moment are equally harmonic functions of τ .

$$\begin{vmatrix} bF(\tau) \\ M(\tau) \end{vmatrix} = \begin{vmatrix} b\tilde{F} \\ \tilde{M} \end{vmatrix} e^{ik\tau}$$

and the linear relation ship between forces and motion is defined by a complex matrix $\mathcal{K}(ik)$:

$$\begin{vmatrix} bF \\ M \end{vmatrix} = -\pi\rho V_0^2 b^2 L \left[\mathcal{K}(ik)\right] \begin{vmatrix} h \\ \theta \end{vmatrix}$$

The complex coefficients of the matrix are designated by the notation :

$$\mathcal{K} = \begin{bmatrix} K_a & K_b \\ M_a & M_b \end{bmatrix}$$

with :

$$K_a = K_a' + i K_a'' \quad , \quad K_b = K_b' + i K_b''$$

$$M_a = M_a' + i M_a'' \quad , \quad M_b = M_b' + i M_b''$$

The model should be a system of differential equations analogous to equations (6), but linear with respect to all its variables, since the problem to which the model applies is itself linear.

The following points will be used to reduce the number of coefficients to be identified :

a) The evolution of the matrix $\mathcal{K}$ as a function of k is smooth and continuous, and can therefore be restored with a single negative pole. As a result the equations in ϕ_r will be limited to the 1st order.

b) Provided that the reduced frequency is low enough, one has $K_b' \simeq K_a''/k$ and $M_b' \simeq M_a''/k$ In the present model, one will assume their strict equalities. Moreover this is true at the limit $k = 0$.

c) Identification and checking of the model will be carried out in the range of the reduced frequency $0 < k < 1$.

The system of equations relating the lift force and moment to the variables of position is denoted by :

$$\begin{vmatrix} bF \\ M \end{vmatrix}^{\cdot} + \underline{\lambda} \begin{vmatrix} bF \\ M \end{vmatrix} = -\pi\rho V_0^2 b^2 L \left[\underline{\lambda} \begin{bmatrix} r_F & s_F \\ r_M & s_M \end{bmatrix} \begin{vmatrix} \theta + h \\ \dot{\theta} \end{vmatrix} + \begin{bmatrix} \delta_F & s_F \\ \delta_M & s_M \end{bmatrix} \begin{vmatrix} \dot{\theta} + \dot{h} \\ \ddot{\theta} \end{vmatrix} \right] \qquad (7)$$

To determine the coefficients of the matrix $\mathcal{K}$, it suffices to proceed by identification after having replaced h, θ, F and M respectively by $\tilde{h}e^{ika}$, $\tilde{\theta}e^{ika}$, $\tilde{F}e^{ika}$ and $\tilde{M}e^{ika}$. One has :

$$K_a' = k^2\lambda \frac{r_F - \delta_F}{\lambda^2 + k^2} \quad , \quad K_b' = r_F - k^2 \frac{r_F - \delta_F}{\lambda^2 + k^2}$$

$$M_a' = k^2\lambda \frac{r_M - \delta_M}{\lambda^2 + k^2} \quad , \quad M_b' = r_M - k^2 \frac{r_M - \delta_M}{\lambda^2 + k^2}$$

$$K_a'' = k\left[r_F - k^2 \frac{r_F - \delta_F}{\lambda^2 + k^2} \right] , \quad K_b'' = k\left[s_F - \lambda \frac{r_F - \delta_F}{\lambda^2 + k^2} \right]$$

$$M_a'' = k\left[r_M - k^2 \frac{r_M - \delta_M}{\lambda^2 + k^2} \right] , \quad M_b'' = k\left[s_M - \lambda \frac{r_M - \delta_M}{\lambda^2 + k^2} \right]$$

To identify the coefficients, one notes that :

- r_F and r_M are the stationary values of K_b' and M_b' .
- K_b'' and M_b'' tend respectively towards $k s_F$ and $k s_M$ at high k .

The 2nd remark leads to determine s_F and s_M in terms of K_b'' and M_b'' at high frequen-

cies (k of the order 1). Whereas the pole $-\lambda$ will be deduced from the variations at low frequency.

Finally, the Mach number is taken as a parameter. In considering the aerodynamic coefficients of the reference 9 at Mach 0.7, identification has led to the following numerical values :

$$\lambda = 0.1 \; ; \; \Gamma_F = 2.801 \; ; \; \Delta_F = 1.65 \; ; \quad \Gamma_F - \delta_F = 1.25 \; ; \quad \Gamma_M = 0 \; ; \quad \Delta_M = 1.6 \; ; \quad \Gamma_M - \delta_M = 0.$$

The results are presented in figures 3.1 to 3.4. Figures 3.1 to 3.3 show the coefficients K_a, M_b and the sum $K_b + M_a$ which determine the aerodynamic effects of stiffness and dissipation for an airfoil oscillating about an arbitrary axis.

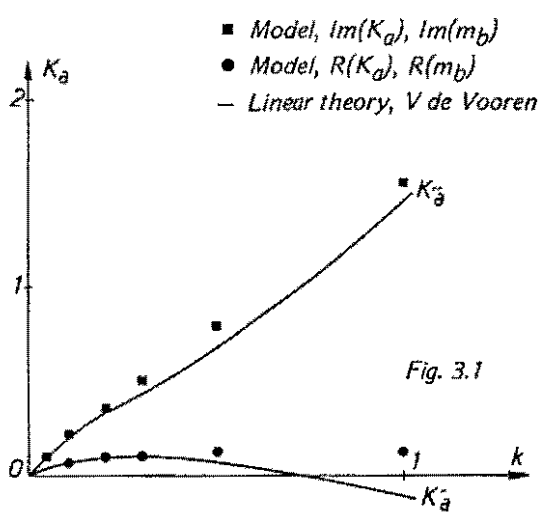

Fig. 3.1

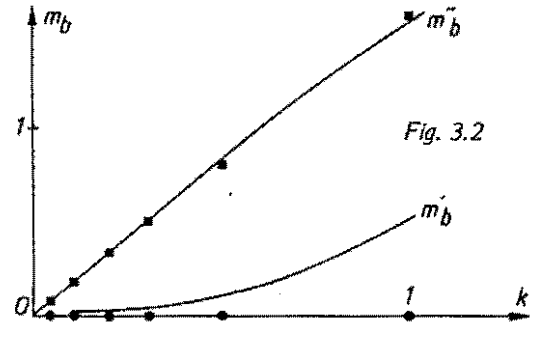

Fig. 3.2

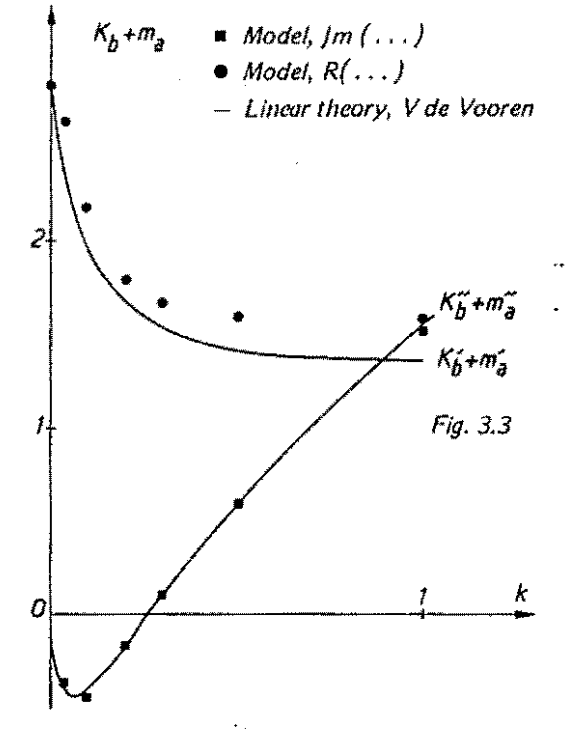

Fig. 3.3

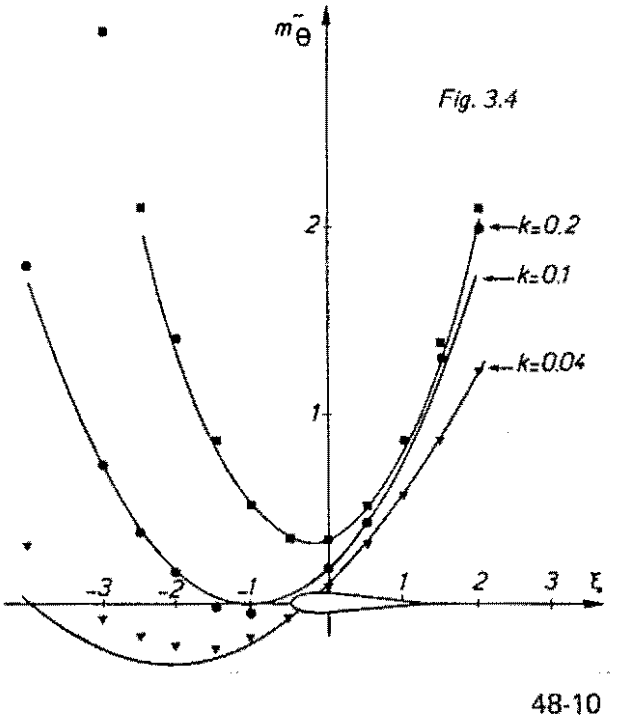

Fig. 3.4

Fig. 3 — Thin airfoil aerodynamic coefficients at Mach 0.7

Fig. 3.1 : K_a - Lift due to heave oscillation.

Fig. 3.2 : m_b - Moment due to pitch oscillation.

Fig. 3.3 : $K_b + m_a$ -

Fig. 3.4 - Moment about the axis of oscillation, imaginary part : $m''_\theta = m''_b + \xi(K''_b + m''_a) + \xi^2 K''_a$.

Figure 3.4 represents the imaginary part of the aerodynamic moment about the axis of oscillation, as a function of the location of this axis and of the reduced frequency of oscillation. The coefficient M''_θ determines the dissipated aerodynamic power.

These results show that the model interprets well the principal tendencies revealed by the linear theory. The discrepancies observed on the coefficients K'_a and M'_b concern the effects of pseudo-elastic and pseudo-inertial forces, which, being small compared with the structural elastic and inertial forces, thus have no significant consequence on the aeroelastic behaviour of the structure.

3. HELICOPTER AIRFOIL SECTION AT HIGH INCIDENCE

The measurements of lift and pitching moment on a helicopter airfoil section oscillating at different amplitudes and frequencies about various mean incidences have been used to validate the model.

The axis of oscillation in pitch is located at the fore-quarter chord line, and the movement is defined by the pitch angle θ. The vector $\vec{V}$ is constant and is confounded with $\vec{V_o}$, and one has :

$$\alpha = \theta \quad ; \quad \vec{V} = \vec{V_o} \implies \sigma = 1 .$$

Tests at small amplitude oscillations are used to identify the model which is then confirmed by tests at high amplitude motions.

The model describing either lift or moment involves a single equation of the 3rd order with a right hand side dependent on the single variable θ .

The measurements of lift and moment have led to the following remarks :

a) For harmonic oscillations at low incidence, that is in the linear regime, evolutions of the measured coefficients in terms of the frequency are smooth and continuous, as shown in the example of paragraph 2.

b) On the contrary, when the mean incidence is higher than the flow separation incidence, rapid variations appear which can only be simulated by two complex poles.

From these remarks, one deduces that the model should possess a real negative pole and two complex conjugate poles. However, the difficulty in this case consists in bringing into play the two complex poles only in the stall regime. This problem has been solved by simply introducing two auxiliary unknowns, which results then in an equation admitting a real pole and an equation giving two complex-conjugate poles.

Let $F(\zeta)$ be the lift or moment function for an unsteady motion defined as a function of ζ .

In stationary flow, F depends only on θ . One has : $F = F_o(\theta)$

The static characteristic $F_o(\theta)$ is composed of two domains : the linear domain, for $\theta < \theta_c$, where $F_o(\theta) = F_{o\ell}(\theta)$ and the stall domain (fig. 4). Let ΔF_o be the difference between the linear characteristic $F_{o\ell}(\theta)$ extended up to the maximum incidence, and the true characteristic

$F_o(\theta)$.

One has

$$\Delta F_o = F_{o\ell}(\theta) - F_o(\theta)$$
$$= 0 \quad \text{for} \quad \theta \leq \theta_c$$

Let us write :

$$\dot{F}_1 + \lambda F_1 = \lambda F_{o\ell} + (\lambda \Delta + \delta)\dot{\theta} + \Delta \ddot{\theta} \tag{8.1}$$

$$\ddot{F}_2 + 2\alpha\gamma \dot{F}_2 + \gamma^2(1+\alpha^2) F_2 = -\gamma^2(1+\alpha^2)\left(\Delta F_o + c \frac{d\Delta F_o}{d\sigma}\right) \tag{8.2}$$

$$F = F_1 + F_2 \tag{8.3}$$

The left hand side of (8.1) determines the real and negative pole ($-\lambda$), and the left hand side of (8.2) determines the two complex-conjugate poles ($-\alpha\gamma \pm i\gamma$).

By eliminating F_1 and F_2 , equations (8) can be reduced to a single 3rd order equation in conformity with (6). Nevertheless, it is preferable to preserve the equations in the form (8.1) to (8.3).

In assuming all time derivatives vanish, one recovers the static limit : $F = F_{o\ell} - \Delta F_o = F_o(\theta)$

Finally, if the airfoil remains at low incidence, $\theta < \theta_c$, (fig. 4, $\Delta F_o = 0$) one retains equation (8.1), consistent with equations (7) (for $k = 0$) which determine the lift and moment in the linear domain of the preceding paragraph. In this domain, it was seen that only a single real pole was needed.

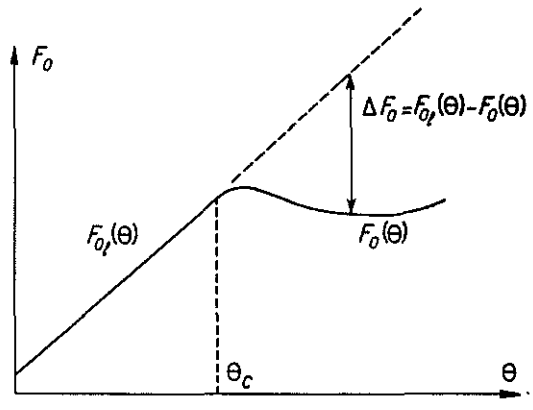

Fig. 4 – Static characteristic of lift.

In what follows one will find a description of the airfoil testing configurations, the details of the identification of the model based on small amplitude harmonic and random oscillations, and the confrontation of the model with experiments at high amplitude motions.

3.1. Test Configurations

Three sets of experiments on two different airfoils had been performed in view of identification of the model.

a) The 1st two sets of experiments were conducted by the Centre d'Essais Aéronautiques de Toulouse (CEAT) on two helicopter airfoil sections, OA212 and OA209, ref. 10, designed by the Aerodynamic Department of ONERA in collaboration with the SNIAS. The airfoils, driven by a linkage mechanism, executed forced simple harmonic oscillations in pitch about the fore-quarter chord. Differential pressure transducers were installed at the central chord section of the airfoils. The overall lift and moment coefficients were obtained by integration of the chordwise pressures, averaged over about six cycles.

The tests configurations were defined by the various combinations of the following different data :

- Oscillation frequencies f = 4, 8, 12 Hz for large amplitude motions.
  = 10, 15, 20, 25, 30, 35, 40 Hz for small amplitude motions.
- Free stream Mach numbers M = 0.12, 0.2, 0.3.
- Airfoil mean incidences θ_o = 0°, 6°, 9°, 10°, 11°, 12°, . . . 19°, 20°, 21°.
- Oscillation amplitudes $\tilde{\theta}$ = 1°, 3°, 6°.

The reduced frequency k and the reduced time τ for a sinusoidal movement :

$$\theta = \theta_o + \tilde{\theta} \cos 2\pi f t$$
$$= \theta_o + \tilde{\theta} \cos k\tau$$

are defined by :

$$k = \omega b / V \ , \quad \omega = 2\pi f \ ; \quad \tau = Vt/b$$

where b is the half chord, t the time, $V = aM$ the flow velocity of the free stream, and a the speed of sound.

Figures 5.1 to 5.4 illustrate, for small amplitude ($\tilde{\theta}$ = 1°) harmonic oscillations in both the linear and stall regimes, typical experimental evolutions of the real part (in phase with the motion), and the imaginary part (in quadrature with the motion) of the normal lift C_N and pitching moment coefficients C_M , as a functions of the reduced frequency k .

Consistent with a convention more commonly used, figures 5 and all those that follow have the airfoil nose-up direction, for positive incidence and pitching moment.

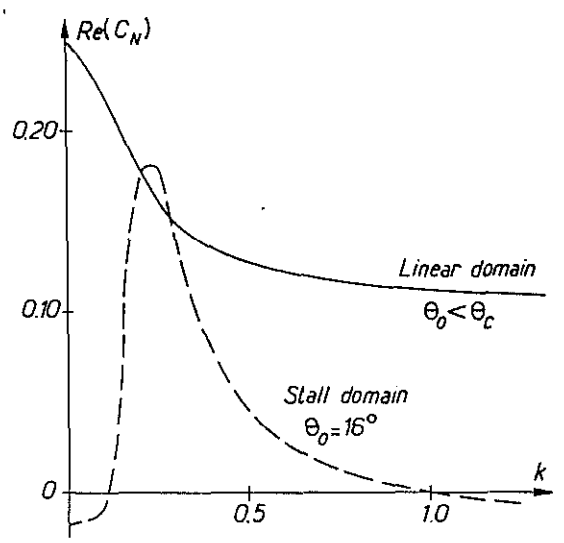

Fig. 5.1 – Real part of the lift coefficient.

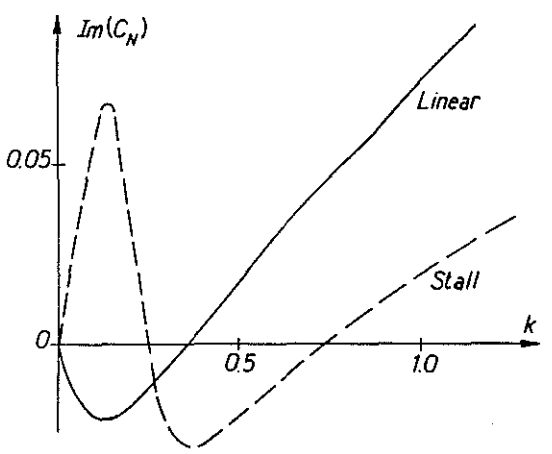

Fig. 5.2 – Imaginary part of the lift coefficient.

Fig. 5 – Typical evolutions of the normal lift and moment coefficients as functions of reduced frequency.

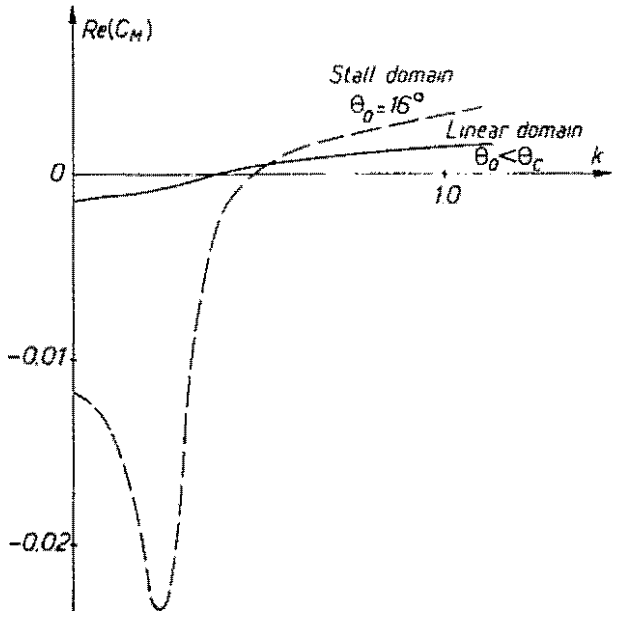

Fig. 5.3 – Real part of the moment coefficient.

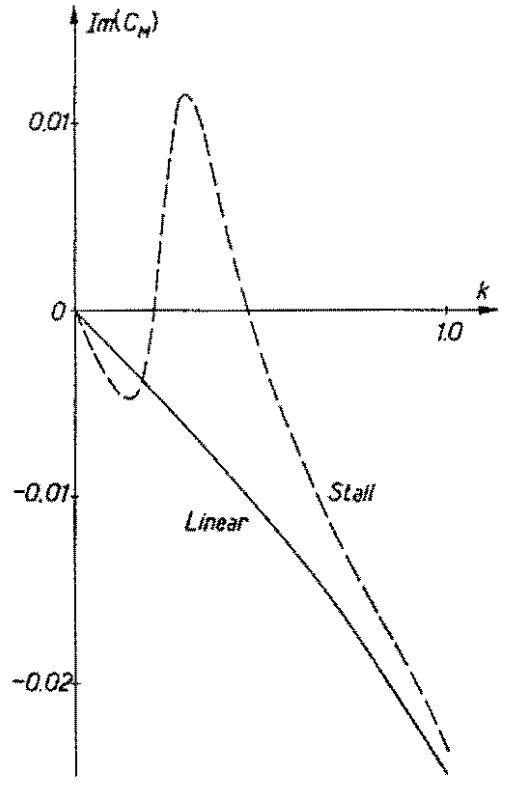

Fig. 5.4 – Imaginary part of the moment coefficient.

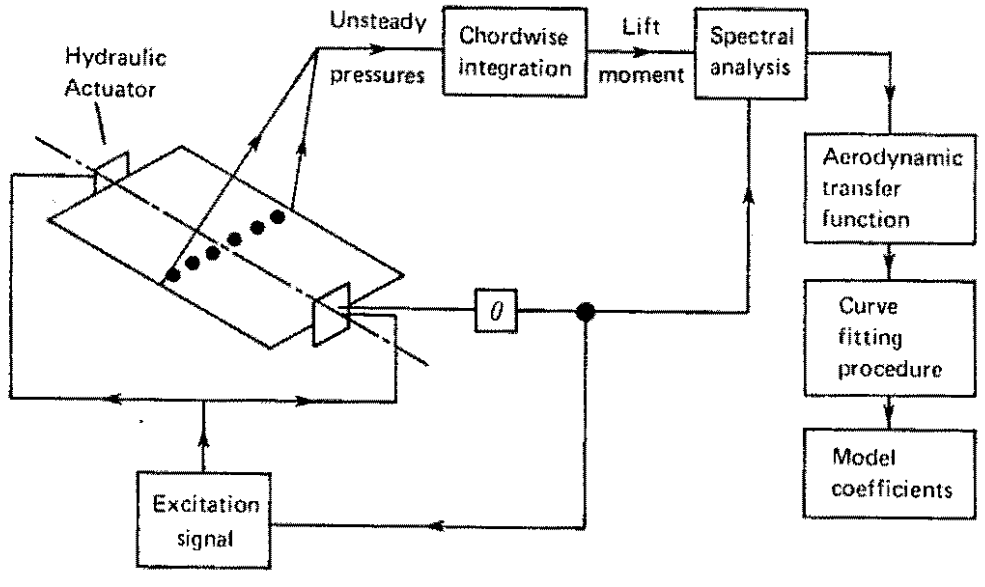

Fig. 6 – Model identification procedure.

b) The third set of experiments was undertaken by ONERA (11) at the S3 Modane wind-tunnel on a 5/8 scale helicopter profile OA209.

The drive mechanism is a hydraulic actuator which (fig. 6) is piloted by an input signal and imposes an arbitrary motion to the airfoil. Tests at small amplitude harmonic and random oscillations in pitch were performed, and the aerodynamic transfer function was obtained by spectral analysis of the input and output signals. For a stationary random process, the aerodynamic transfer function or admittance $A(i\omega)$ is defined as the ratio of the cross power spectral density $\Phi_{f\theta}(\omega)$

of the output $f(t)$ – input $\theta(t)$, to the power spectral density $\Phi_{\theta\theta}(\omega)$ of the input Thus

$$A(i\omega) = \frac{\Phi_{f\theta}(\omega)}{\Phi_{\theta\theta}(\omega)}$$

with $\Phi_{f\theta}$ and $\Phi_{\theta\theta}$ respectively the Fourier transforms of the cross correlation function $\varphi_{f\theta}(t)$ of the output-input, and of the autocorrelation function $\varphi_{\theta\theta}(t)$ of the input :

$$\Phi_{f\theta}(\omega) = \int_{-\infty}^{\infty} \varphi_{f\theta}(t) e^{-i\omega t} dt \quad , \quad \Phi_{\theta\theta}(\omega) = \int_{-\infty}^{\infty} \varphi_{\theta\theta}(t) e^{-i\omega t} dt$$

and

$$\varphi_{f\theta}(t) = \lim_{T\to\infty} \frac{1}{2T} \int_{-T}^{T} f(u+t)\,\theta(u)\,du$$

$$\varphi_{\theta\theta}(t) = \lim_{T\to\infty} \frac{1}{2T} \int_{-T}^{T} \theta(u+t)\,\theta(u)\,du$$

The output $f(t)$, as a function of time, is then given by the convolution integral :

$$f(t) = \int_{-\infty}^{\infty} a(u)\,\theta(t-u)\,du$$

where $a(t)$ is the impulsive response function, defined as the inverse Fourier transform of the transfer function of the system :

$$a(t) = \frac{1}{2\pi} \int_{-\infty}^{\infty} A(i\omega) e^{i\omega t} d\omega$$

Tests at small amplitude random oscillations about given mean incidences are particularly useful since, for a given mean incidence, the transfer function $A(i\omega)$ can be obtained through one single experiment in the whole range of reduced frequency of interest.

Figures 7.1 to 7.4 show comparisons between the experimental transfer functions measured by a random oscillation process (ONERA) and by harmonic oscillations at discrete frequencies (ONERA and CEAT) on the OA209 airfoil. The harmonic oscillation results are fairly consistent. Further more, the relatively good agreement of the results obtained through random and harmonic oscillations confirms the validity of the principle of superposition in the case illustrated.

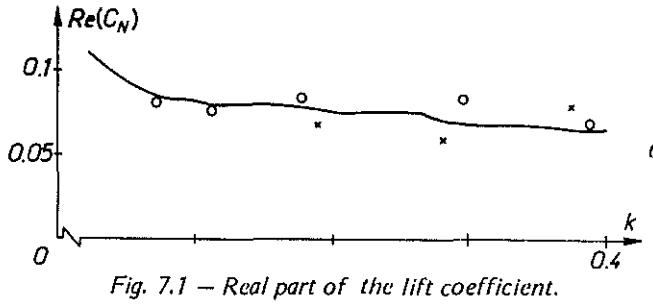

Fig. 7.1 – Real part of the lift coefficient.

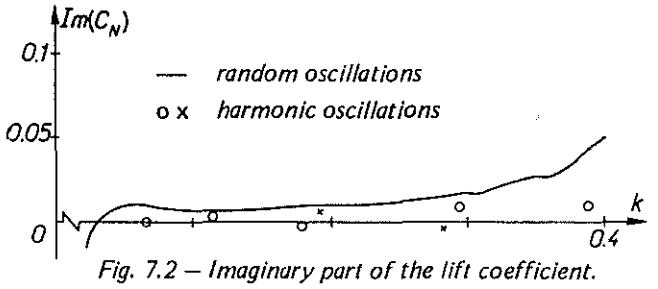

Fig. 7.2 – Imaginary part of the lift coefficient.

Fig. 7 – Comparison of lift and moment coefficients resulting from small amplitude harmonic and random oscillations in the wind-tunnel S3 of Modane.

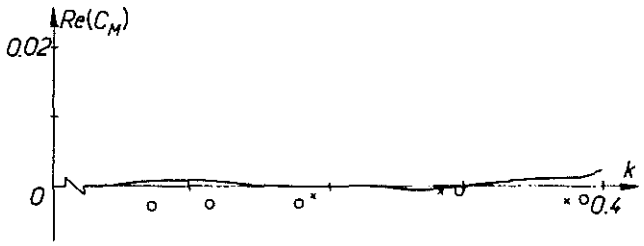

Fig. 7.3 – Real part of the moment coefficient.

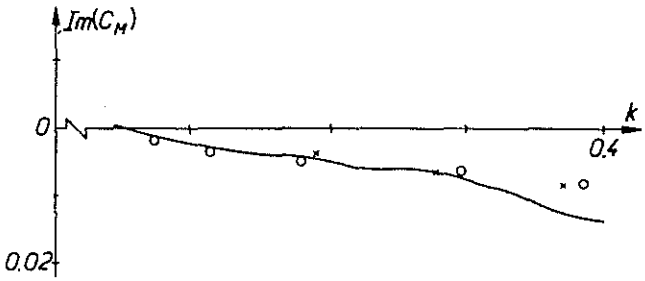

Fig. 7.4 – Imaginary part of the moment coefficient.

3.2. Identification of the Model through Tests at Small Amplitude Motions

For small amplitude ($\tilde{\theta} \leqslant 1°$) sinusoidal pitch oscillations of the airfoil, the aerodynamic coefficients C_N and C_M are also practically sinusoidal in shape. Indeed, the relative amplitudes of the higher harmonics are negligible – of the order of 1/10 of the fundamentals – in the whole range of mean incidences θ_0 and reduced frequencies k of the tests. This property is important in the identification process since it gives a formal solution corresponding to a sinusoidal motion.

Thus, for small amplitude oscillations of the airfoil : $\theta = \theta_0 + \tilde{\theta}\cos kt = \theta_0 + \tilde{\theta}\,\mathcal{R}e^{ikt}$, with $\tilde{\theta} \leqslant 1°$.

The coefficients C_N or C_M , denoted by F , are written in the form :

$$F = F_1 + F_2 = F_0 + \mathcal{R}\tilde{F}e^{ikt} = (F_{01} + F_{02}) + \mathcal{R}(\tilde{F}_1 + \tilde{F}_2)e^{ikt}$$

with $\tilde{F}$, $\tilde{F}_1$ and $\tilde{F}_2$ complex.

The real and imaginary parts of equations (8) then read :

$$\mathcal{R}(\tilde{F}) = \left[\frac{dF_{0\ell}}{d\theta} - \frac{k^2\left(\frac{dF_{0\ell}}{d\theta} - \delta\right)}{\lambda^2 + k^2}\right]_{\theta_0}\tilde{\theta} + \left[\frac{\gamma^2(1+\alpha^2)\frac{d\Delta F_0}{d\theta}}{\left(k^2 - \gamma^2(1+\alpha^2)\right)^2 + 4\alpha^2\gamma^2k^2}\right]\left[k^2(1-2\alpha\gamma c) - \gamma^2(1+\alpha^2)\right]_{\theta_0}\tilde{\theta} \tag{9.1}$$

and

$$\mathcal{I}(\tilde{F}) = k\left[1 - \frac{\lambda\left(\frac{dF_{0\ell}}{d\theta} - \delta\right)}{\lambda^2 + k^2}\right]_{\theta_0}\tilde{\theta} + k\left[\frac{\gamma^2(1+\alpha^2)\frac{d\Delta F_0}{d\theta}}{\left(k^2 - \gamma^2(1+\alpha^2)\right)^2 + 4\alpha^2\gamma^2k^2}\right]\left[c\left(k^2 - \gamma^2(1+\alpha^2)\right) + 2\alpha\gamma\right]_{\theta_0}\tilde{\theta} \tag{9.2}$$

In the following remarks, the physical significance of the notations employed in equations 8 and 9 are indicated :

– $F_o(\theta)$ denotes the static characteristic of either the lift or the moment coefficient as a function of incidence θ . The equations in the present model make no distinction between the static characteristics and the constant parts of lift or moment coefficients resulting from small amplitude oscillations. Experimental results, however, show that vibration does have a non linear effect which tends to increase the mean values of the outputs with respect to the corresponding static values. This effect can not be taken into account except by introducing the appropriate non-linearities in the model. Here, $F_o(\theta)$ is as a matter of fact, an allowable compromise between the « true » static characteristics, and the measured mean values in small amplitude oscillations.

– $(dF_{o\ell})/(d\theta)$ is the slope of the static characteristic in the linear domain : $\theta < \theta_c$, where θ_c is the static stall incidence.

– $\Delta F_o(\theta)$ represents the difference between the extented linear static characteristic and the real static characteristic : $\Delta F_o(\theta) = H(\theta-\theta_c)\left(F_{o\ell}(\theta)-F_o(\theta)\right)$
H being the unit step function.

The parameters :
– λ , real negative pole, or time delay parameter ;
– $\delta\tilde{\theta}$ slope of the imaginary part at high frequency k ;
– $\delta\tilde{\theta}$ asymptote of the real part at high frequency k ;
– α reduced damping coefficient associated with the complex pole,
– γ reduced circular frequency of « resonance » associated with the complex pole,
– C variable which causes a phase shift of the output in the regime beyond the stall incidence

are a priori, functions of the mean incidence θ_o and of the Mach number M .

In examining the set of families of curves generated by each term of equations (9), and by comparing with the experimental results in both the linear and stall regimes, one sees that the experimental transfer functions in the whole range of mean incidence can be described by superposition of the two solutions (9.1) et (9.2) of the present model.

The procedure of identification is handled differently in the linear domain and in the stall regime.

Linear Domain : $\theta_o < \theta_c$

The mean incidence is below the static stall angle : $\Delta F_o = 0$. The periodic solution F_2 of equation (8.2) is identically zero, and the outputs of lift and moment are given by (8.1) alone. In this domain, the evolution of the experimental transfer functions, figures 5, are smooth and continuous, resembling those given by the classical linear theories of Küssner, V. de Vooren, Theodorsen, etc. The numerical values of $(dF_{o\ell})/(d\theta)$, λ , δ and δ can be identified with no difficulty in this case.

Stall Domain : $\theta_o > \theta_c$

The mean incidence is higher than the static stall angle : $\Delta F_o \neq 0$, and $(d\Delta F_o)/(d\zeta) \neq 0$. The experimental results show the apparition of a complex pole, whose imaginary part, or « resonant frequency » is a function of θ_o (figures 5). The buffeting, characterised by a continuous

spectrum caused by the random fluctuation of the flow, can evidently not be simulated by a single pole. On the contrary, a continuous spectrum suggests a continuous distribution of poles in the frequency domain, which can only be treated with the use of statistical mechanics. It is admitted that there is only one single complex pole, whose imaginary part is $\gamma(\theta_0, M)$, and whose real part is the aerodynamic reduced damping $-\alpha\gamma(\theta_0, M)$. These two parameters, together with the coefficient C, determine the response F_2 in the stall regime.

The identification procedure in the stall regime is somewhat more delicate. By the character of the differential equations, the transfer function or admittance, equations (9) written in the complex form $A(ik) = P(ik) / Q(ik)$ is a rational fraction, with P and Q both polynomials in ik, and the poles are given by the zeros of the denominator $Q(ik)$. Identification of the coefficients by a classical least square curve fitting procedure leads inevitably to a set of non linear equations. However, the optimisation process can be made linear by adopting a method analogous to that given in ref. 12, which, in defining a special error norm, is particularly suited for optimising transfer functions in the form of rational fractions, as those occuring in most structural problems.

The present identification process can be applied to all Mach numbers, provided that no new phenomenon, such as transonic effects, arises and comes to alter profoundly the behaviour of the response as a function of the reduced frequency.

Two identifications have been accomplished so far on the OA212 airfoil at Mach number M = 0.12 et 0.3. By interpolation and extrapolation of the coefficients so obtained, the model can be extended from the incompressible case to Mach = 0.4.

3.3. Large Amplitude Harmonic Oscillations

The model identified in the manner indicated in the paragraph 3.2 has been applied to large amplitude harmonic oscillations.

Consider the system of differential equations (8) with variable coefficients dependent on an input of sinusoidal motion. At small amplitude oscillations, equations (8) can be linearized about the mean incidence, which leads to a system of equations with constant coefficients. The solution can be obtained with no difficulty in this case. At high amplitude oscillations, the periodic variation of the coefficients in terms of the instantaneous incidence must be taken into account. The situation results then in a system of equations with periodic coefficients dependent on a periodic input, and the solution in such cases is obtained through the Floquet theory.

In each application, the asymptotic stability of the system must be ensured.

In applying the periodicity condition, the periodic solutions for lift and moment are evaluated by integration over one single period of oscillation.

The model has been applied to the whole set of test configurations on the OA212 airfoil at large amplitude harmonic oscillations in pitch. The various test cases, 141 in all, comprise the variations of Mach number, mean incidence, amplitude and reduced frequency of oscillation.

Figures 8 and 9 present the comparisons calculation – experiment on the evolution of lift vs. incidence and moment vs. incidence hysteresis loops, as a function of mean incidence θ_o varying between 0° and 17° all other parameters being kept fixed : amplitude of oscillation $\tilde{\theta}$ = 6°, reduced frequency k = 0.05 and Mach number M = 0.3.

At low incidence (figs 8.1 and 9.1), the unsteady flow remains attached in the linear domain, the lift and moment hysteresis loops both take the form of an ellipse. The ellipses have their respective centres located on the static characteristics. Their eccentricities, and in the case of lift, the sense of gyration, are function of the reduced frequency k . From the evolution of the real and imaginary parts of lift and moment as a function of k , (figures 5), one can deduce that as k progressively increases from the static value zero, the lift-incidence ellipse, whose eccentricity begins with the value 1, gradually fills out, then flattens again when the imaginary part $\Im(C_N)$ crosses the k axis. From there on the ellipse fills out once more, and takes on an opposite sense of gyration. However, the moment – incidence ellipse conserves the same sense of gyration throughout the whole range of frequency, due to the constant sign of its imaginary part.

At relatively larger mean angles of attack, the instantaneous incidences overlap both the linear and stall regimes, the lift and moment hysteresis loops tend to take on respectively the form of an 8 (figs 8.3 to 8.6), and of an $\backsim$ (figs 9.3 to 9.6). These characteristics, similar to those described in reference 13 as the stall onset and light dynamic stall, imply that the responses are made up of a number of non negligible higher harmonics. One notices that the lower branch of the lift hysteresis corresponding to incidences lower than the static stall angle, conserves a more or less

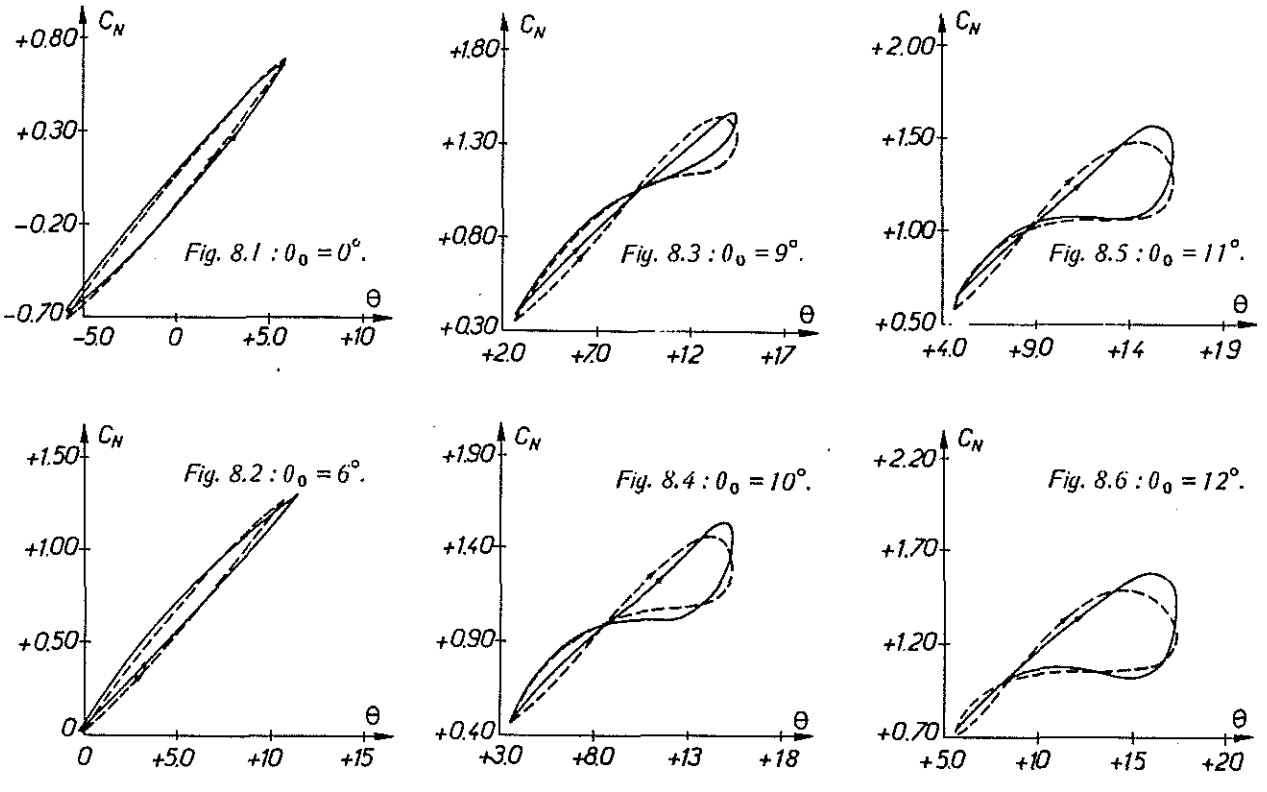

Fig. 8 – Large amplitude harmonic oscillations ; influence of the mean incidence on the lift-incidence hysteresis loop. Mach 0.3 ; reduced frequency : 0.05 ; oscillation amplitude : 6°.

— Experiment ; - - - model ; > sense of gyration.

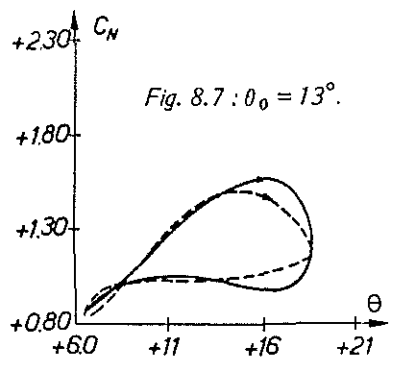

Fig. 8.7 : $\theta_0 = 13°$.

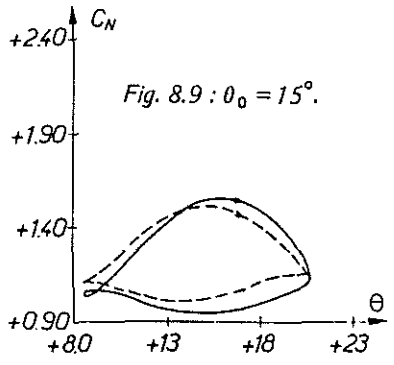

Fig. 8.9 : $\theta_0 = 15°$.

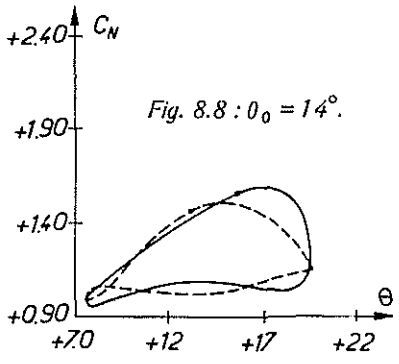

Fig. 8.8 : $\theta_0 = 14°$.

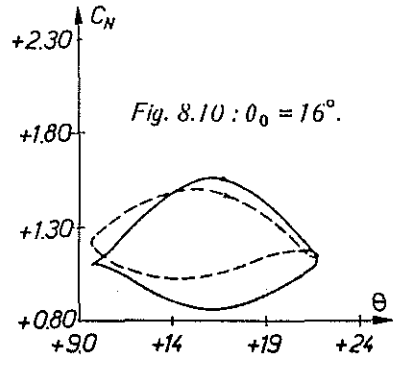

Fig. 8.10 : $\theta_0 = 16°$.

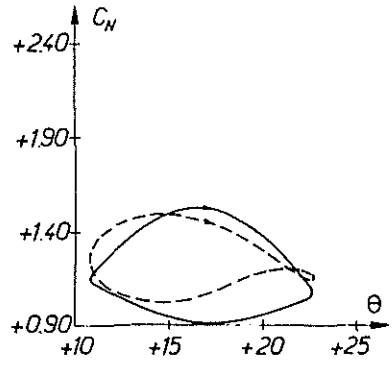

Fig. 8.11 : $\theta_0 = 17°$.

deformed elliptical form, with the same sense of gyration as in the linear case. These deformations originate from the participation in the total response, of the transient damped solution of the homogeneous periodic coefficient equation (8.2). The same remark applies equally to the moment hysteresis, and the curvature in the central part of the moment loops is due to the static moment characteristic, which curves up at still moderate incidence before its abrupt break.

As the instantaneous incidence increases ($\dot{\theta} > 0$), and passes beyond the static stall angle, dynamic stall takes place only after a certain delay such that the unsteady lift attains much greater values than the corresponding static lift. Mean while, the pitching moment magnitude remains moderate. Similarly, as the instantaneous incidence, starting from the static stall angle, decreases ($\dot{\theta} < 0$) down to the linear range, flow reattachment does not take place instantaneously, so that the unsteady lift takes on values lower than the corresponding static lift. Such phenomena are well known (14), and are due essentially to the effects of delay and the acceleration and deceleration of the flow in a pitching motion.

At much higher incidence (figures 8.7 to 8.11 and 9.7 to 9.11) the lower branch of the lift hysteresis disappears progressively, and one observes the onset of the pitching moment break. In the last 3 cases (figures 8.9 to 8.11 and 9.9 to 9.11), the boundary layer being totally separated, the lift hysteresis loops take on the form of a two pointed cocked hat, with a sense of gyration opposite to that of the linear case, and the pitching moment hysteresis loops resemble deformed rectangles enclosing the static moment curve.

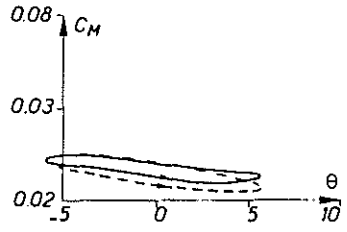

Fig. 9.1 : $\theta_0 = 0°$.

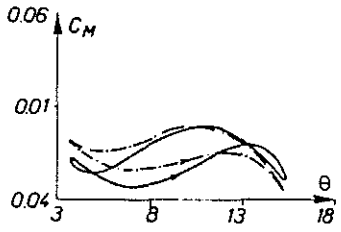

Fig. 9.4 : $\theta_0 = 10°$.

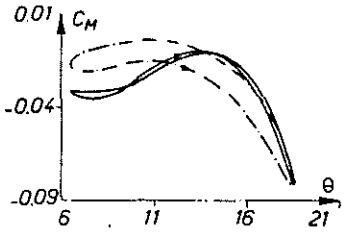

Fig. 9.7 : $\theta_0 = 13°$.

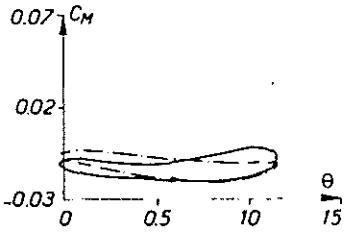

Fig. 9.2 : $\theta_0 = 6°$.

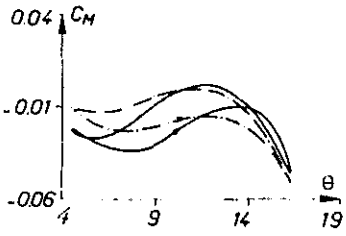

Fig. 9.5 : $\theta_0 = 11°$.

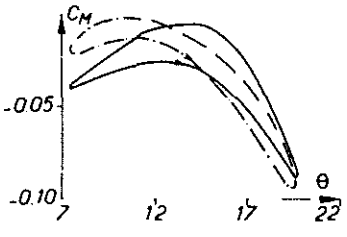

Fig. 9.8 : $\theta_0 = 14°$.

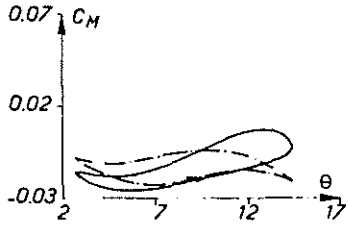

Fig. 9.3 : $\theta_0 = 9°$.

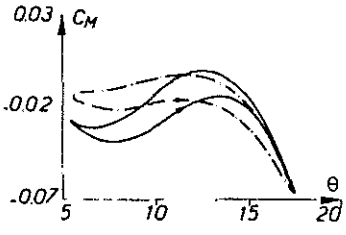

Fig. 9.6 : $\theta_0 = 12°$.

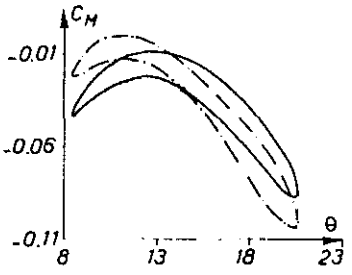

Fig. 9.9 : $\theta_0 = 15°$.

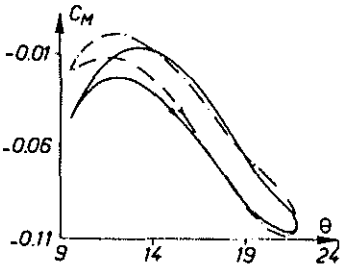

Fig. 9.10 : $\theta_0 = 16°$.

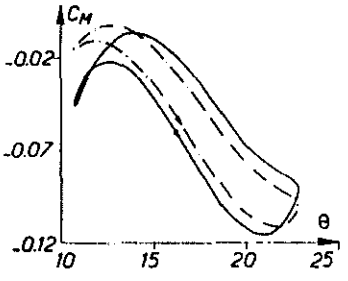

Fig. 9.11 : $\theta_0 = 17°$.

Fig. 9 — Large amplitude harmonic oscillations ; influence of the mean incidence on the moment-incidence hysteresis loop. Mach 0.3 ; reduced frequency : 0.05 ; oscillation amplitude : 6°. — Experiment ; ---- model ; > sense of gyration.

CONCLUSION

The use of a system of differential equations enables the introduction of the effects of time history of the flow in a logical manner, and to interpret the principal tendancies revealed both by the exact theory, in the linear domain, and by the wind-tunnel experiments in the regime of high incidences. In spite of the simplifications brought to the model in order to facilitate its identification and its use, the comparisons between model and experiment, and model and exact linear theory are satisfactory.

Furthermore, the formulation in the form of differential equations presents the following advantages :

– The model can be applied to all arbitrary motions of the airfoil, defined as a function of time.

– The model can be incorporated with no difficulty in the set of equations governing the aeroelasticity of a rotor.

The only hypothesis that needs to be postulated in order to justify the general form of the model (equation 3) consists in admitting the differentiability of the operator determing the aerodynamic forces as a function of the variables defining the motion of the airfoil. One can then deduce that the model should be valid over a wide range of conditions, notably at high Mach numbers, excepting the extremely critical situation where an infinitesimal variation of incidence can induce a finite variation of lift or moment

REFERENCES

1. R.E. Gormont — *A Mathematical Model of Unsteady Aerodynamics and Radial Flow for Application to Helicopter Rotors.* Boeing Vertol Company. A.D. 767240. Prepared for AAMRDL. May 1963.
2. D.W. Gross, F.D. Harris — *Prediction of Inflight Stall Airloads from Oscillating Airfoil Data.* 25th Annual National Forum of the American Helicopter Society. Washington. May 1969.
3. T.S. Beddoes — *A Synthesis of Unsteady Aerodynamic Effects Including Stall Hysterisis.* 1st European Rotorcraft and Powered Lift Aircraft Forum. Southampton. September 1975.
4. J.J. Costes — *Calcul des forces aérodynamiques instationnaires des pales d'hélicoptère.* Rech. Aérosp., n° 1972-2.
5. R. Dat — *Aérodynamique instationnaire des pales d'hélicoptère.* Table ronde sur l'Aérodynamique instationnaire de l'AGARD, Göttingen. 30 mai 1975.
6. J.J. Costes — *Introduction du décollement instationnaire dans la théorie du potentiel d'accélération. Application à l'hélicoptère.* Rech. Aérosp., n° 1975-3.
7. R. Dat, C.T. Tran, D. Petot — *Modèle phénoménologique de décrochage dynamique sur profil de pale d'hélicoptère.* XVI° Colloque d'Aérodynamique Appliquée (AAAF). Lille, novembre 1979.
8. D. Favier, J. Repont, C. Maresca — *Profil d'aile à grande incidence animé d'un mouvement de pilonnement.* XVI° Colloque d'Aérodynamique Appliqué (AAAF). Lille, novembre 1979.

9. A.I. Van de Vooren — *Collected Tables and Graphes of Theoretical Two-dimensionnal, Linearized Aerodynamic Coefficients for Oscillating Airfoils.* NLR Report F 235.

10. J. Coulomb — *Moyen d'essais pour l'étude d'écoulements instationnaires autour de profils en oscillation d'incidence.* XIV^{e} Colloque d'Aérodynamique Appliquée (AAAF). Toulouse, novembre 1977.

11. E. Szechenyi — ONERA Report to be published.

12. R. Dat, J.L. Meurzec — *Exploitation par lissage mathématique des mesures d'admittance d'un système linéaire.* Rech. Aérosp., n° 1972-4.

13. W.J. McCroskey et al. — *Dynamic Stall on Advanced Airfoil Sections.* 36th Annual Forum of the American Helicopter Society. Washington, D.C. May 1980.

14. E. Lars, Ericson et al. — *Unsteady Airfoil Stall.* Lockheed Missiles and Space Company, Sunyvale, California, July 1969 (NASA CR 66787).